Energy & Geoscience Institute

Geochemical Monitoring of the Coso Geothermal System

September, 2005- Prepared for the Geothermal Program Office at the China Lake Naval Air Weapons Station

by

Michael C. Adams

under

Contract # N68936-02-C-0206

TABLE OF CONTENTS

EXECUTIVE SUMMARY 6

TASKS AND PROGRESS SUMMARY 7

3.1: Task 1: Chemical Analysis: 7

3.2: Task 2: New Resource Areas 7

3.3: Task 3: Coso Hot Springs 7

3.4: Task 4: Additional Investigations 8

INTRODUCTION 9

CHEMICAL MONITORING OF THE COSO FIELD 10

Review 10

Current Year 12

2004 Chemical Data 12
Data Consistency 12
Injection locations, quantities, and chemistry 12
NaKCa Geothermometer Temperatures 12
NaKCa Geothermometer Temperature Trends 13
Quartz Geothermometer Temperatures 13
Quartz Geothermometer Temperature Trends 14
Reservoir Boiling (Excess Steam) 14
Chloride Concentrations 15
Chloride to Boron Ratios 17
Quartz-NaKCa temperature differences 17

COSO HOT SPRINGS 17

Review 17

Recent Data 18

ADDITIONAL INVESTIGATIONS 18

Carbon-14 dating of the travertine on the East Flank 18

Possible causes of the elevated silica in the Coso production waters 19

Chemical modeling of augmentation waters 23

REFERENCES 24

Appendix I - Summary of the Conductive Heating Results 29

LIST OF FIGURES

Figure 1. Injection locations and quantities during 2004.

Figure 2. Location of wells that produced single-phase steam during 2004.

Figure 3. Average ratio of chloride to boron in the injection fluids during 2004.

Figure 4. Average chloride concentration(ppm) in the injection fluids during 2004.

Figure 5. NaKCa geothermometer temperatures (^{o}C) during 2004.

Figure 6. Percent change in the NaKCa geothermometer temperatures from 2003 to 2004.

Figure 7. A simple qualitative evaluation of trends in the NaKCa geothermometer temperatures in recent years.

Figure 8. A more detailed qualitative evaluation of NaKCa geothermometer temperature trends.

Figure 9. Quartz geothermometer temperatures (^{o}C) during 2004.

Figure 10. Percent change in the quartz geothermometer temperatures from 2003 to 2004.

Figure 11. A simple qualitative evaluation of trends in the quartz geothermometer temperatures in recent years.

Figure 12. A more detailed qualitative evaluation of quartz geothermometer temperature trends.

Figure 13. Excess steam fractions during 2004.

Figure 14. Percent change in the excess steam fractions from 2003 to 2004.

Figure 15. Chloride concentrations (ppm) during 2004.

Figure 16. Percent change in the chloride concentrations from 2003 to 2004.

Figure 17. Qualitative evaluation of chloride concentration trends in recent years.

Figure 18. Chloride to boron ratios during 2004.

Figure 19. Percent change in the chloride to boron ratio between 2003 and 2004.

Figure 20. A comparison of the wells in which the quartz geothermometer temperature is greater than that of NaKCa during 2004 with the 2003 data.

Figure 21. Isotopic variation of the water from well 4P-1 since 1979.

Figure 22. Isotopic variation of the water from well 4K-1 since 1993.

Figure 23. Isotopic variation of the water from well 4K-1 since 1993. Composition of rain (upper red circle) and snow (lower red circle) during Jan 2005 sampling season are shown for comparison.

Figure 24. Isotopic variation of steam and liquid from Devil's Kitchen since 1974.

Figure 25. Isotopic variation of the water from the Nicol Prospect since 1974.

Figure 26. Isotopic variation of the mudpots and pools along the Coso Fault since 1974.

Figure 27. Isotopic variation of the water from West Canyon since 1993.

Figure 28. Isotopic variation of the South Pool since 1989.

Figure 29. Isotopic variation of the Navy II fumarole since 1995.

Figure 30. Schematic representation of how elevated silica concentrations may precede thermal breakthrough of injection water. The graph is a plot of temperature versus saturation for typical injection waters.

LIST OF TABLES

Table 1. Isotopic data from Coso Hot Springs wells and fumarolic pools around the producing field. 18

Table 2. Results of carbon-14 dating of pollen extracted from the East Flank travertine. The samples were analyzed by accelerator mass spectrometry at the Rafter Radiocarbon Laboratory located in Lower Hutt, New Zealand.....19

EXECUTIVE SUMMARY

This document illustrates the geochemical changes that took place at the Coso geothermal field during the year 2004. Thematic maps from the Coso Geographic Information System show the yearly changes in chloride, geothermometer temperatures, excess steam, and chloride-to-boron ratios as well as their actual values. These plots indicate that:

1) reservoir cooling rates are within reasonable limits for a geothermal system of this magnitude;
2) chloride changes are consistent with surface boiling from power production and injection recycling, except for northwest Navy I and the western edge of Navy II and BLM West. In these cases there appears to injection recycling of condensate and an influx of peripheral geothermal water, respectively.
3) The silica increases that occurred over the last few years are abating. Fewer wells are showing this phenomenon that the prior year for the first time in 5 years.

The annual sampling and analysis of the stable isotopes of water occurred in January. Despite some possible small contamination by rain and snow, the analyses show that the activities of the surface manifestations remains constant.

Carbon-14 dating was performed on pollen extracted from the interior of two samples of the East Flank travertine. The samples underwent extensive pretreatment to remove any possible contamination. The results indicate that the travertine was active approximately 12,000 years ago, just within the last glacial episode. These dates are much younger than the uranium disequilibrium age of 307,000 years. The C-14 procedure is much simpler and is not model-dependent, in contrast to uranium disequilibrium dating.

TASKS AND PROGRESS SUMMARY

3.1: Task 1: Chemical Analysis:

The Contractor shall update the established geochemistry database of all Coso geothermal system geochemical analyses from brine and gas samples.

The raw data provided to the contractor were recalculated to the composition of the liquid as it entered the well bore. An analysis from each well in the field that still produces liquid was provided by the contractor, and was included in the recalculation if the quality of the analysis was sufficient (see below).

The Contractor shall both compile and evaluate the quality of the data using (previously established) protocols.

The quality of the data was evaluated using the charge balance, the amount of air accidentally included in the gas sample, and the consistency of the analysis with previous samples. The quality of the data was high, with the exception of a few bad charge balances.

The Contractor shall update the established geochemistry database on a yearly basis and continue the established time-trend analyses of indicator constituents to include but not limited to chloride, boron, enthalpy, and appropriate geothermometers.

GIS representations of the indicator constituents were prepared for the year 2004. GIS representations of the change in these constituents were also prepared and historical trends for the relevant constituents are included as graphs for each well.

The Contractor shall conduct 4-D geochemical modeling of production field fluids (brines and gases) to track changes occurring in the reservoir due to production and injection activities. The Contractor shall conduct enthalpy mapping and through that, assess injection efficiencies in the geothermal field.

Steam fractions and their changes (i.e., enthalpy mapping) over the last few years are included as GIS coverages.

3.2: Task 2: New Resource Areas

The Contractor shall conduct a geochemical characterization of new fluids from adjacent exploration areas, specifically the Navy's deep test holes…including both brine and gas sampling.

No samples were obtained or provided.

3.3: Task 3: Coso Hot Springs

The Contractor shall update the established Coso Hot Springs geochemistry database on a yearly basis and continue the established time-trend analyses of (previously established) indicator constituents. This shall be done in order to monitor the geochemical nature of the hot springs

and to continue to evaluate possible relationships between the fluids produced at the hot springs and those present elsewhere in the Coso geothermal system.

The Coso Hot Springs spreadsheet database was updated with the isotopic compositions determined from samples taken during January, 2005. The data were added to the hot springs Access database file. The file "Coso Hot Springs.mdb" contains only stable isotope data and a copy is included on the companion CD of this report.

3.4: Task 4: Additional Investigations

The Contractor shall investigate, recommend, and apply new techniques and processes which will contribute to the Navy's basic understanding of the geochemistry of the Coso geothermal system, particularly the relationship of reservoir fluids to host rock, source rock, heat source, reservoir conduits (plumbing), other physical parameters, and time.

Samples of the East Flank Travertine were sent out for Accelerator Mass Spectrometry carbon-14 age dating. The dates appear quite young at about 11,800 years BP.

The ongoing investigation of the elevated silica concentrations found in some of the production fluids continued this year. The problem appears to be decreasing. A summary of the relevant literature on geothermal quartz and amorphous silica chemistry is included.

Assistance was provided to Dr. Bruce Christenson (IGNS: Institute of Geological and Nuclear Sciences, Ltd.) on an investigation of the chemical evidence for a magmatic source of some components of the Coso geothermal fluids.

Fluid-mineral chemical modeling of the reservoir fluid and its possible interaction with augmentation water was continued this year. This work was initiated as a reservoir monitoring tool under this contract, but has been continued as a permeability scaling research tool using funding by the DOE-EGS program. A summary of the progress of the current set of simulations is included in this report.

The Contractor shall also recommend additional measurements that might be made in the future to further clarify both the source and rate of movement of fluids found in and around the Coso Hot Springs Resort, and to better define the relationship between the fluids in the Resort area and the commercial Coso geothermal reservoir.

No recommendations are suggested by the data at this time.

INTRODUCTION

This document is the third yearly report for the current contract on the geochemical monitoring of the Coso geothermal field. The major sections of this report reflect the tasks listed in the current contract: the health of the producing field and Coso Hot Springs, new techniques to improve monitoring the same, and research that adds to knowledge of the geothermal system and its history.

The Coso geothermal system is located on the China Lake Naval Air Weapons Station (NAWS) in southeastern California. Fluid from the geothermal system has been used to produce up to 270 MW of electricity since 1988, which has considerably offset the cost of electricity used at NAWS, and lowered its dependence on conventional energy sources. The process of energy production from a geothermal system as large as that found at Coso involves the extraction and reinjection of massive quantities of water. The resulting changes in the fluid mass and physical state of the reservoirs will, in turn, lead to chemical changes as temperatures are altered and minerals dissolve and precipitate. The recognition and quantification of the chemical changes and trends that develop plays an important role in guiding field development and exploitation strategies.

This study has two major objectives. The first is to define and interpret any chemical changes that have occurred in the Coso reservoir as a result of production, and to correlate these changes with productivity problems such as excessive reservoir boiling. The components of this task include data acquisition, processing, storage in a relational database, and display in a geographic format. The results of this work provide methodologies and algorithms to interpret the data derived from any geochemical monitoring programs sponsored by the Navy in the future.

The second objective of this project is to monitor the geochemical indicators of activity at the Coso Hot Springs, and to evaluate the relationship between the hot springs and the deeper reservoir currently being exploited for power production. The Coso Hot Springs Resort is on the National Register of Historic Places and is under the stewardship of the NWC under the Code of Federal Regulations (CFR Title 36, Chapter I, 60.4 effective 1 April 1976). Concerns over its preservation had arisen because of the increase in activity displayed by the hot springs in 1988, which may eventually threaten the historic structures near the hot springs. Geochemical monitoring provides a method of evaluating changes in the hydrologic system that feeds the Coso Hot Springs.

In the following sections, the research that has been performed in support of these objectives during prior contract years will be reviewed, followed by a discussion of the current work.

CHEMICAL MONITORING OF THE COSO FIELD

Review

A database system that contains the raw analyses of water and gas from the Coso field was set up during the four years of the first contract. The database system ports the data through a processing program, which performs the following functions: 1) culls the raw data for bad charge balances and air contamination, 2) calculates geothermometer temperatures, 3) correlates water and gas analyses, 4) uses the geothermometer temperatures and measured enthalpy to compensate for concentration changes due to boiling and excess steam, and 5) calculates parameters such as the excess steam fraction and the geothermometer enthalpies. The final product is itself a database. The algorithms for the quartz geothermometer and the excess steam calculation were refined during the third year of the contract to accommodate the high temperatures found within the East Flank reservoir. The cation geothermometer used in the database was switched from the NaK (Fournier, 1981) to the NaKCa (Fournier and Truesdell, 1973) for the same reason.

The database has been used to create thematic maps of the chloride concentrations, geothermometer temperatures, and reservoir boiling. The purpose behind the thematic maps is to monitor and document any changes in the reservoir chemistry resulting from exploitation. Reservoir chemistry changes can indicate the incursion of cooler waters (Ellis and Mahon, 1977), the flow of injected water, which is required for pressure maintenance (Stefansson, 1997), and the excessive flow of injection water, which would cool parts of the reservoir too quickly. The choice of the parameters was derived from several discussions in the literature of observed and theoretical chemical changes in exploited geothermal reservoirs (Abrigo et al., 2002; Ellis and Mahon, 1977; Harper and Jordan, 1985; Henley, 1984a; Henley, 1984b). The data were averaged to determine the change in these parameters for each year since 1989. During the first three years of the contract, the various parameters were contoured on plan maps to emphasize the trends, but are now presented as classified points. The change was implemented to avoid the assumptions of continuity inherent in contouring.

The functionality of the monitoring database was greatly increased by joining it to a geographic information system (GIS) of the Coso geothermal field during the fourth year of the first contract. A map of the field was digitized using the computer program ARC/INFO. Seven coverages were created: 1) well courses, 2) well heads, 3) production intervals, 4) well pads, 5) roads, 6) unit boundaries, and 7) section lines. The location of the production intervals were chosen by picking the highest density of lost circulation zones along the well course. If the density distribution was uniform, the midpoint of the well course was chosen. The data are stored in geographic coordinates (latitude and longitude; decimal degrees) and have been projected to the 1927 California State Plane, Zone IV, for display on the figures.

The database processing programs were rewritten during the last contract in the more modern computer language Visual Basic. The programs were rewritten to interact

with the database program Microsoft Access rather than Paradox. Access is the database that the operators of the Coso field use to store and manipulate their data. The purpose behind the reprogramming was to increase the number of tasks automated by the program, and to provide greater compatibility with the field operator's databases. For example, each year the contractor provides the chemical data to us in a different format. This necessitated a lengthy examination and reformatting of the spreadsheet and database. The new programs make the transition easier.

The GIS coverages were redone last contract using CAD files obtained from the Coso contractor. The coverages used in previous reports were based on paper copies of the well locations, which was the only form provided to us by the Coso contractor. This paper-copy method of creating coverages is inaccurate, and was considerably improved by using the CAD files.

Two new features were added to the plots in the last report of the last contract. The first is the identity of the dry steam wells. These wells, for which there are no liquid analyses, have no geothermometer or chloride values to show on the plots. The spread of dry steam wells is a negative indicator for the "health" of the field, so they are now shown on the plots (by red triangles). Their abundance in the northern portion of the plots demonstrates why there are few liquid analyses in Navy I. The second feature added to the plots is the location and annual amount of each injection well in million pounds per year. This allows a comparison of the index constituents with the injection pattern.

The emphasis of the evaluation was changed to examination of individual wells during the first year of the current contract. This was changed because the sampling schedule has been regularized so that all wells are sampled once per year, rather than frequent but irregular sampling that was the hallmark of previous years. This approach facilitates a qualitative evaluation of the trends for each well. These trends are noted on a map from the Coso geochemical GIS. To support this approach a plot is provided for each well with the five parameters used to evaluate the "health" of the well.

The significance of the Cl/B ratio was examined in detail and this parameter was added to the four that were previously used. The significance of rising silica concentrations in the production water was also investigated. The cause of the rising silica continues to be problematic and is reexamined this year.

GIS plots were added that show the distribution and magnitude of the silica increase by displaying wells in which the quartz geothermometer temperature is greater than that of NaKCa. The points are classified with respect to the magnitude of the gap.

Two other new plots are the injection concentrations of chloride and the injection ratio of Cl/B. These provide perspective on the communication of the injection and production wells.

Current Year

2004 Chemical Data

A total of 50 wells produced only steam in 2004. Forty-five wells produced steam and liquid. All of the wells were sampled. Eight of the two-phase wells lacked a measured enthalpy, and eight had charge balances that exceeded +/- five percent. The analyses with bad charge balances were incorporated into the database after being examined for obvious problems in the index constituents. None were found, and the analyses were used.

Nine wells have excess steam fractions of less than 10%. All of the two-phase samples were taken on the same date as the total enthalpy was measured. This improves the utility of the data immensely.

Data Consistency

Historical trends of the index parameters that are used to monitor the field were examined for consistency. All of the data for NaKCa, quartz, chloride, Cl/B, and excess steam were plotted versus time for the wells sampled during 2004. The plots were examined for any trend reversal or increased scatter over the last few years. In general, the trends were consistent and there was no more scatter than during previous years. An exception to this was noted in the last few reports. Although the problem was not widespread, several wells showed more excursions in their quartz temperatures than in previous years. This effect peaked last year, and the high quartz concentrations are now decreasing. This is discussed in more detail later in this report.

Injection locations, quantities, and chemistry

Injection locations and quantities are shown in figure 1. The only significant difference from prior years is injection into well 88-1. This well is located in a portion of the field that may allow more much-needed injection into Navy I. The locations of the 2004 steam wells are shown in figure 2. Figure 3 shows the average ratio of chloride to boron in the injection waters. This ratio can vary widely day to day, depending on the fraction of condensate in the injectate. The average concentration of chloride in the injection waters is shown in figure 4. The geographic distribution of chloride remains high in the south and low in the north.

NaKCa Geothermometer Temperatures

NaKCa geothermometer temperatures (Fournier and Truesdell, 1973) can be used to monitor temperatures in regions away from the well bores because of the slower equilibration rate of this geothermometer. If general reservoir cooling occurs or a cooler fluid is being drawn in, advance warning may be given by changes in the NaKCa geothermometer temperatures.

The NaKCa temperatures for the Coso waters during 2004 are shown in Figure 5. This figure shows that there has been no change in the distribution of temperatures in

the field, i.e., no intrusion of cooler waters or excessive cooling due to injection breakthrough.

NaKCa Geothermometer Temperature Trends

Figure 6 shows the change during the last year in the NaKCa geothermometer temperatures. With the exception of seven wells, the NaKCa geothermometer temperatures did not vary by more than 3% during the last year. Four of the outliers increased, while three decreased; all less than 10%. The outliers are dispersed throughout the field, and seem to be random fluctuations. Three percent is within the "normal" rate of decrease i.e., that documented by previous reports in this series and consistent with comparable geothermal systems (Abrigo et al., 2002).

Visual examination of the NaKCa data for each well was used to produce plots that show the overall trends. The most recent four samples (usually representing the last four years) were weighted most heavily when considering the trends. This technique was used to produce two plots. The first, shown in figure 7, is a simplified version in which the trends are divided into decreasing temperatures (down), no change (even), increasing temperatures (up), and erratic data (jumpy). This longer-term view shows that most of the wells are decreasing, although a few remain at relatively constant temperatures.

A more detailed analysis of the trends divides the wells into categories of accelerating temperature decreases (acc), constant decrease (const), no decrease (even), decelerating temperature decreases (deacc), or erratic data (jumpy). This is shown in figure 8. This view also indicates that the temperature decrease is constant, and not accelerating.

The NaKCa and quartz geothermometer temperatures as well as chloride, excess steam, and the Cl/B ratio are shown versus time for each well as jpg files in the accompanying CD.

Quartz Geothermometer Temperatures

The quartz geothermometer is quick to equilibrate at geothermal reservoir temperatures (Fournier, 1981). It reflects temperature changes closer to the well bore than the NaKCa geothermometer. It can be used to monitor changes such as cooling due to reservoir or local boiling, or an imminent flux of cooler waters.

The quartz temperatures in the Coso production waters are shown in Figure 9. The north-south and east-west temperature zonation is still clearly indicated by this geothermometer, similar to that shown by the NaKCa geothermometer temperatures. Figure 10 shows the yearly changes in the quartz geothermometer temperatures for the period 2003-2004. In contrast to the previous few years, in which quartz temperatures were rising in a large fraction of the wells, they are now decreasing or increasing at a rate less than 3% per year.

Although there does not appear to be a "silica problem" anymore, possible reasons for rising silica were investigated and the implications of rising silica are discussed in more detail in the section "Additional Investigations".

Quartz Geothermometer Temperature Trends

The long-term quartz trends were difficult to evaluate, having now reversed in a number of wells. Overall, they seem to be heading downwards again. Figures 11 and 12 show these trends. A number of the wells are defined as "jumpy" because of the reversal in direction.

Reservoir Boiling (Excess Steam)

The amount of steam that hot water produces can be calculated from the enthalpy of water at any given temperature. However, the situation is more complicated in many geothermal wells. Restricted permeability around the well or low wellhead pressures will produce steam outside of the well bore. Since steam flows much more rapidly than liquid, especially when the fraction of steam is large, the steam will reach the well ahead of its associated liquid. This results in the enthalpy of the total discharge increasing. Eventually, if unchecked, the liquid will never reach the well bore. This is the case when a well goes "dry".

There are several reasons why an operator may wish to prevent wells from going dry:

1) Localizing the boiling interface may result in mineral precipitation in a restricted portion of the reservoir, lowering permeability around the well.

2) Producing liquid and recirculating it through injection spreads out the thermal drawdown in the reservoir. Producing only steam provides much less water to reinject, limiting the opportunity to draw heat from the whole reservoir.

3) Hydrochloric acid can be produced in the steam of high-temperature wells that have dried out (Adams, unpublished data). This can lead to dangerous conditions unless the wellhead and pipeline conditions are closely controlled to prevent condensation of an acid liquid. The Coso contractor is aware of this and monitors the wells for HCl production.

4) If no liquid is produced, the information derived from chemical monitoring is strongly restricted. For example, temperature declines in the reservoir, changing sources of the water, and recharge rates and directions of injectate cannot be determined.

The excess steam plot for 2004 is shown in figure 13. This plot shows that almost all of the wells in Navy I produced dry steam during 2003, while the few remaining two-phase wells were generally low in excess steam. BLM unit wells are mixed; most of the wells in BLM West had high excess steam fractions, while BLM East had low to moderate quantities of excess steam. About a third of the wells in the East Flank had greater than 70% excess steam.

The changes in excess steam production are shown in Figure 14. This plot shows the absolute change in excess steam fraction, in percent, rather than a relative percentage change. The fraction of excess steam stayed constant in about half the wells in all units throughout the field. Two thirds of the remaining wells stayed constant, while the others showed decreases.

Chloride Concentrations

The chloride concentrations are shown in Figure 15. The gradient continues to trend from low salinities in the north and east to high salinities in the southwest. The percentage change in the chloride concentrations are shown in Figure 16. In general, concentrations of all non-volatile elements in geothermal waters are increased by boiling at the surface before injection. The concentration increases at Coso range from 20 to 30%, and vary depending on the amount of injection being recycled in any given well. Chloride is a conservative (non-reactive) element, and monitoring its increase in the production waters is one relatively inexpensive way of monitoring the spread of injected waters. This method is most effective when the production waters are uniform, providing a good baseline for the production wells and a uniform source of water for the injection wells. Unfortunately, there is a range of chlorinity in the production waters at Coso and the composition of the injection waters change frequently. These difficulties render the chloride monitoring method qualitative, rather than quantitative technique as used by Sullara and Horne (1999; 2001).

The use of chloride to examine injection connectivity was improved last year, although it is still qualitative. The average concentration of injection was added to the plot, allowing comparison of the injection and nearby production concentrations (Fig. 15). This allows one to determine which should go up and which should go down, i.e., if a well has high chloride near a low-chloride injection well, the production chloride should go down. There are several cases where some of the nearby wells are greater than the injection chloride, and some are less. This helps explain the apparently inconsistent juxtaposition of increasing and decreasing chloride concentrations.

Each cluster of injection and production wells was examined in this way. Note that conclusions can not be made on the absolute mass transfer between the wells, only on whether the chemistry is dominated by that of the injection water. In addition, wells "drying out" can be influenced by reservoir boiling, which can increase chloride and decrease the Cl/B ratio.

Cluster 1. Injection wells 24A-8, 61B-7, 54-7, and 88-1RD. As with last year, all of the production wells in this area have an average chloride that is less than or equal to that of the injection wells. Despite this, they all show a decreasing or level chloride concentration, shown in the 2004-2003 chloride change (Fig. 16) and in the overall trends (Fig. 17). This is confirmed by the Cl/B ratios (Fig. 18) and the Cl/B trends (Fig. 19). The injection wells all have Cl/B ratios greater than or equal to the production wells, yet most the production wells are going down.

It would appear that these wells are mixing with a fluid that is low in chloride and low in the Cl/B ratio. Condensate would satisfy these requirements, either reservoir condensate from the steam zone in Navy I or an injection well that is not obvious condensate using yearly averages. Alternatively, there may be an influx of peripheral fluid that is lower in Cl and Cl/B ratio.

Cluster 2. Injection well 23-17 and the production wells west and southwest of the injection well. The injection chloride in this area is less than the production chloride (Fig. 15), and the production trends are going down (Figs. 16 and 17). The Cl/B data

is inconclusive (Figs. 18 and 19). It may be that injection well 23-17 does not reach the wells west of it. The decreasing Cl/B south of well 23-17 is consistent with it having some influence to the south.

Cluster 3. Injection wells 67B-17, 67C-17 and 86-17 and the production wells west and southwest of the injection wells. In this cluster the injection well chloride concentrations are similar to or lower than those of the production wells (Fig. 15). This year the nearby production wells are decreasing in chloride (Figs. 16 and 17), while those further away are increasing. This probably indicates a strong contribution from the southern injection wells in section 20 to those wells that are further away (cluster 5). The Cl/B data is consistent with this conclusion. The injection ratios are similar to or lower than most of the nearby production ratios, and the production ratios showed a decrease or no change in 2004 (Figs. 18 and 19).

Cluster 4. Injection wells 58-18, 23A-19, and 46A-19 and the five production wells that lie between or near these wells. The injection well chloride is higher than those of the production wells (Fig. 15). The production well chloride went down or was even during 2004, indicating that the injection well does not have a dominating effect on the chemistry of the wells (Figs. 16 and 17). The Cl/B ratios should have gone up if dominated by that of the injection well, but instead held steady (Figs. 18 and 19). Excess steam is high in these wells, so that the directions could have been influenced by reservoir boiling.

Cluster 5. Injection wells 46-19, 46A-19, 47A-20, 47B-20, 68-20RD, 68A-20RD, 68B-20, and 88-20RD and the production wells northeast of the section 19 wells and northwest of section 20 wells. Chloride in the injection wells is dominantly greater than that in the production wells (Fig. 15). This year most of the nearby production wells show a trend towards gently increasing or steady chloride. This trend extends northward to Cluster 3 (Figs. 16 and 17). The Cl/B values of the injection and production wells are very similar near the southern injectors, so little change would be expected. However, like last year, some of the wells display a shift to high Cl/B ratios, even higher than that of the injection waters (Figs. 18 and 19). This also occurs in Cluster 3. This is something of a mystery, as these wells have Cl/B ratios of 65 to 92, whereas the injection wells do not exceed 55. This might imply that these wells are drawing from a portion of the reservoir untainted by the injection wells, or with extremely high Cl/B ratios. Of course, there is always the possibility of analytic error. However, the alignment of the wells in a straight line may imply communication between these wells.

Cluster 6. The East Flank. Injection wells 64A-16, 83-16, 51B-16, and 34A-9 and all of the production wells in the East Flank. Chloride concentrations in the East Flank are increasing for all two-phase production wells that were sampled with the exception of 38C-9 (Figs. 15-17). This is consistent, as chloride concentrations are higher in the injection wells than the production wells. The Cl/B is similar in the injection and the production wells, and there is quite a bit of excess steam in the East Flank (Figs 13-18). Thus, the Cl and Cl/B method is not very useful in this area.

Chloride to Boron Ratios

A new index constituent was added last year, the ratio of chloride to boron in the liquid phase. The rationale and systematics of its use were explained under last year's additional investigations. The correlation of Cl/B between injection and production wells is summarized in the chloride section, above. In this section I will merely note the distribution of the ratio at Coso during 2004.

The highest ratios are in BLM East and the lowest in Navy I, Navy II and the East Flank. This distribution roughly reflects the ratios in the initial state system. In detail there are more ratios below 34 than in the initial state, caused by the development of steam zones. Production and injection have also lowered ratios in fluids from the western edge of BLM West to values expected from Navy I and II. This may also be due to an influx of peripheral geothermal fluids, which tend to have lower Cl/B and Cl. However, ratios in BLM East remain at the high values (45-65) expected for this area, reflecting the initial composition, the injectate composition, and the abundance of injection wells in the southeastern corner of this region.

Quartz-NaKCa temperature differences

Rising silica concentrations have prompted an additional series of plots in this report. Figures 20 shows the differences between the geothermometer temperatures for this year superimposed over those for last year. The significance of these plots is discussed below, in the Additional Investigations section.

COSO HOT SPRINGS

Review

Coso Hot Springs is a prominent feature of the Coso area. Its buildings and mud pots are both an historical landmark (CFR Title 36, Chapter I, 60.4 effective 1 April 1976) and a Native American religious site. Concern was raised about the stability of the hot springs area when its activity began to increase during the late 1980's. This increase in activity came on the heels of the Navy I unit being brought on line, prompting speculation that the two events were related. Pressure drops caused by geothermal production have been known to dry up hot springs and increase fumarolic activity in other localities (Ellis and Mahon, 1977; Stefansson, 1997). EGI was contracted by the Navy in 1993 to address these concerns using chemical and isotopic methods of investigation.

Chemical and isotopic sampling of the hot springs and vicinity were conducted by EGI beginning in 1993. The data showed that significant isotopic shifts had occurred in water and steam from some of the shallow wells (Adams, 1994; Adams, 1995). It was concluded that the most likely cause of the increased activity was a pressure drop caused by exploitation of the field. A pressure drop would have increased the boiling fraction of the water at the hot springs, resulting in the observed isotopic shift.

Pressure drops are a natural result of geothermal exploitation, where 10 to 20% of the produced water is not reinjected (Ellis and Mahon, 1977). Steaming ground such as

that seen near the hot springs and along the Pipeline Road at Navy II fumarole often results from such pressure drops. Isotopic sampling and analysis of the hot springs waters has been continued under this contract to provide some warning in case more activity increases occur.

Recent Data

The stable isotope compositions of the fumarolic pools throughout Coso continued to shift to heavier values only in the case of the South Pool and the wells 4P-1 and 4K-1. The changes are shown in Figures 21 through 29, and the data are listed in Table 1. The isotopic composition of the waters continues to change along the previous trend, both forward and reverse, in most cases. The Nicol prospect water, shown in Figure 25, is reversing the trend for the second year. This is probably due to a lack of injection water input into the pool since injection was stopped in the adjacent 41-8 pad. The other reversals could be due to a cooler, more water-rich year, or to slight admixture of the snow that occurred the day before sampling (Table 1; Figure 23).

Table 1. Isotopic data from Coso Hot Springs wells and fumarolic pools around the producing field.

Sample	$\delta^{18}O$	δD
Devil's Kitchen	-3.26	-78.6
Nicol	-4.14	-83.8
Coso Fault	0.91	-71.8
4P-1	-2.66	-72.3
4K-1	-5.62	-87.4
South Pool	5.47	-63.0
Slump Canyon	-3.2	-84.1
Navy II Canyon	-1.5	-72.3
West Canyon	-0.60	-77.9
Rain, Death Valley	-11.75	-79.0
Snow, Front Gate at Coso	-21.0	-153.1
Wheeler Prospect	-2.66	-89.8

ADDITIONAL INVESTIGATIONS

Carbon-14 dating of the travertine on the East Flank

Pollen extracted from the travertine that lies along the southeastern edge of the East Flank was dated using accelerator mass spectrometry (AMS). Three samples were taken from the travertine. They were taken from the top, the bottom, and near the center where a pod of abundant fossilized twigs was found. The samples were subjected to stringent procedures for removing contamination by modern carbon. At the end of these procedures there was no carbon left to date in the sample from the bottom sample. The dates obtained from the remaining samples ranged from 11,838 to 11,685 years before present, where “present” is 1950. These ages are extremely young when compared to the age of 307,000 years BP obtained by the uranium disequilibrium dating of Leslie and

Hammond (1990). The carbon-14 dates are just within the last glacial episode, so surface outflow and a high water table at that time is not an unreasonable supposition.

Table 2. Results of carbon-14 dating of pollen extracted from the East Flank travertine. The samples were analyzed by accelerator mass spectrometry at the Rafter Radiocarbon Laboratory located in Lower Hutt, New Zealand.

Sample ID	R Number	NZA	$\delta^{13}C$	Radiocarbon Age
Coso 05-3 Mini twigs	28812/7	22218	-26.8	11838 ± 40 BP
R05-1 Top of travertine	28812/8	22219	-27.8	11685 ± 50 BP

Sample ID	$\delta^{14}C$(‰)	$\Delta^{14}C$(‰)	Percent Modern
Coso 05-3 Mini twigs	-773.3 ± 1.2	-772.4 ± 1.2	22.76 ± 0.12
R05-1 Top of travertine	-769.4 ± 1.4	-768.1 ± 1.4	23.19 ± 0.14

NZA 22146-22149, 22180 are provisional results
Pending measurement of delta-c13 values

Calibration for NZA 22218

2 sigma interval is 11850 BC to 11661 BC	13799 BP to 13610 BP (93.1% of area)
1 sigma interval is 11811 BC to 11720 BC	13760 BP to 13669 BP (65.4% of area)

Calibration for NZA 22219

2 sigma interval is 11747 BC to 11442 BC	13696 BP to 13391 BP (97.0% of area)
1 sigma interval is 11681 BC to 11485 BC	13630 BP to 13434 BP (80.3% of area)

Possible causes of the elevated silica in the Coso production waters

As noted in previous reports, silica concentrations rose over the last few years in many of the Coso production waters. The elevated concentrations found in many of the wells have begun to decrease and return to quartz equilibrium this year. These increases were alarming because:

1. The data reduction is carried out by assuming that the water is in equilibrium with quartz;
2. The increased silica could presage increased silica scale or injection breakthrough in the production wells;
3. The change in silica could indicate a change in mineral equilibria in the reservoir, altering the patterns of mineral dissolution/precipitation and thus the permeability distribution.

The cause of the silica rise is uncertain. Although the threat seems to have abated, it seems wise to further examine the possible causes:

Injection. It has long been known that the arrival of the chemical signature of injection water (chemical breakthrough) will precede any temperature drop (thermal breakthrough) (Horne et al., 1987). Increases in silica concentration in production waters have also been predicted to presage thermal breakthrough by some reservoir models that incorporate silica chemistry (Harper and Jordan, 1985; Malate and O'Sullivan, 1991). A schematic explanation of his process is shown in figure 30. The results of these models must be viewed skeptically because of the very poor agreement between kinetics measured in the lab and those observed in the field (Carroll et al., 1998; Zhu, 2005). In these studies it was shown that field rates are 3 to 10 times slower than lab rates. Although injection breakthrough and cooling seem like perfectly reasonable mechanisms to explain the silica increases at Coso, the pattern of increases does not fit the history of injection well locations. For example, BLM West has had the most effective injection returns to production wells, yet is the least affected by silica increases. Similarly, the East Flank has had the poorest record of injection returns, and is the youngest part of the field, but shows some strong increases in silica.

Another possibility is a change in the source region of the water. For example, reservoir boiling could have lead to deeper inflow zones, and higher temperatures. Unfortunately, such mixing would also produce higher cation temperatures, which haven't been seen. A similar explanation has arisen from the silica increases that have occurred at Wairakei, New Zealand. It has been speculated that these increases are due to combination of boiling and mixing with cooler recharge waters in equilibrium with chalcedony (Lovelock, 1995). This does not appear to be the case at Coso, however, as indicated by the otherwise constant cation temperatures and chemistry of the waters. In addition, in many cases it is the hottest waters in the center of the field (e.g., 74B-19) that are showing the most consistent increases in silica. These waters should be the least affected by cool water infiltration.

A third possible cause is acidification of the injection water (pH mod). This practice was first studied by Lawrence Livermore National Laboratory (Grens and Owen, 1977) to combat the scale at the Salton Sea geothermal field. The theory behind pH mod is based on the inhibition of iron silicate and sulfide scale in hypersaline brines. Subsequent studies have extended its use to other fields. Some fields use geothermal gases to lower the pH (Hirowatari and Yamachi, 1990; Klein, 1995), while others inject sulfuric or sulfurous acid (Gallup, 1996; Gallup, 1997; Gallup, 2002). The theory behind its use is that polymerization and condensation of amorphous silica is retarded under acidic conditions. It is possible that this inhibition allows high silica waters to enter the hot reservoir formation, and that equilibrium is never re-established with quartz along the injection-production flow path. This would allow silica oversaturations to persist, i.e., a remnant of the concentration from boiling would remain. This would be consistant with the amount of silica excesses seen in the production fluid. However, quartz kinetics at high temperature should be rapid enough to prevent this, unless there is some other effect of the acidification that is interfering. So, although this explanation seems the most likely, is still problematic.

In addition, there are many convolutions in the kinetics of the silica polymorphs, as described below.

Silica kinetics are a complex topic. The following is a brief description of the process and a literature survey that is far from complete, but is included to give a taste of the large volume of work that has been published on this topic. Two general references on silica not mentioned below are Iler (1979) and Heaney et al. (1994).

Silica Polymorphs

Thermodynamics

The dominant silica minerals in high-temperature geothermal systems are quartz and amorphous silica. Quartz is the least soluble, while amorphous silica is the most soluble. Chalcedony is a polymorph that is frequently found to be in equilibrium with low- and moderate-temperature waters, especially in volcanic terrains (Arnorsson, 1975; Fournier, 1981). The other common polymorphs of silica, cristobalite and trydimite, are not generally found to be in equilibrium with geothermal waters. The solubility of these minerals increases with temperature and pH, and decreases with salinity. The temperature dependence can be described by simple polynomial expressions, as given by Fournier and Rowe (1966), more complex expressions (Fournier and Potter, 1982), or expressions that also give the dependence on salinity as well as temperature (Chen and Marshall, 1982a; Chen and Marshall, 1982b; Fournier, 1983). A recent modification to the low temperature end of the quartz expression is given in Rimstidt (1997).

The solubility of amorphous silica has been of special interest to the geothermal community because this is the polymorph that clogs pipelines and wells, and its solubility appears in its kinetic rate expression. A review of amorphous silica solubility is given in Chan (1989). Recent articles redefining, or slightly modifying, the solubility expressions for amorphous silica have been given by Gallup (1989), Gunnarsson and Arnorsson (2000), and Icenhower and Dove (2000).

Amorphous Silica Kinetics - Deposition from Polymer Colloids

Amorphous silica precipitates by two distinctly different mechanisms. The first is colloidal deposition, which may occur when the solution is oversaturated with respect to amorphous silica by a factor of 10 or more (Log Q/K > 1)(Weres et al., 1982). Colloidal deposition is the result of silicic acid polymerizing in solution, then forming three-dimensional aggregates that are micron-sized (colloids). The time-scale for this is from minutes to days, depending on pH, temperature, surface area, and salinity (Bohlmann et al., 1981; Fleming, 1986; Icopini et al., 2005; Weres et al., 1982). The colloidal particles are then deposited on surfaces and glued together by more silica polymers. This mechanism generally forms bulky, low-density scale, although it can also form the vitreous, high-density version discussed below (Bohlmann et al., 1981). The rate of deposition is influenced by pH, temperature, solution composition, amorphous silica surface area, and flow regime (Carroll et al., 1998; Fleming, 1986; Gallup, 1989; Gallup, 1996; Grens and Owen, 1977; Iler, 1979; Weres et al., 1982).

The most widely-regarded kinetic model for amorphous silica formation has been developed by Fleming (1986). In this model an intermediary is formed, which consists of silicic acid bonded to particles of amorphous silica by a single bond. The

bonding is essentially chemisorption. In this model the novel ingredient is the introduction of silicic acid site occupancy into the rate expression. The model holds the kinetics of interaction between dissolved and chemisorbed silicic acid as independent from any other interaction. The subsequent incorporation of the chemisorbed silicic acid into the three-dimensional bonded network of the amorphous silica is treated in a separate kinetic expression.

Although Fleming's work is regarded as the best model, it doesn't include polymer nucleation or aggregation-and-deposition of the colloidal silica. These processes must be included for any prediction of actual deposition rates. Weres (1982) has presented a model that is more complete, although his kinetic expression does not include the fraction of site occupancy.

Hydrodynamics has been shown to play a role in silica deposition from colloids (Carroll et al., 1998; Dunstall and Brown, 1998). This is particularly applicable to the surface facilities of geothermal fields. The remainder of this paragraph is a description of this process from an unpublished manuscript by Kevin Brown, a New Zealand researcher. "The hydrodynamic conditions control the access of the suspended colloid to the walls of the pipe or other scaling surfaces. The important parameters are the width of the boundary layer, the viscosity of the fluid and the particle characteristics. By definition, for a scale to form, colloids must move from the solution to the walls, and this means that the particles must pass through the boundary layer… Certainly, it is noticed that silica scaling is more likely on bends and other areas where the boundary layer is altered. As well, we have noticed that highly turbulent flow (i.e., large Reynold's number) tends to cause an increase in silica scaling."

Amorphous Silica Kinetics - *Deposition from Monomers*

The second mechanism by which amorphous silica can be deposited is direct deposition from monomeric silicic acid. Molecular deposition occurs when the growing polymer surface is a solid rather than a colloid suspended in solution. Silicic acid and silicate ions migrate by circulation and diffusion to the solid surface. The rate of deposition is a function of temperature, supersaturation, and the density of silinol groups ionized to $–Si-O^-$ on the solid growth surface. The effective surface density increases with salinity and, of course, pH (Weres et al., 1982). Molecular deposition is primarily responsible for producing hard, vitreous, often dark colored scale, with density of about 2.1 to 2.3 g/cc. Rates of direct deposition on amorphous silica have been measured by far fewer researchers than the crystalline silica phases. The most relevant citations to geothermal applications are Bohlmann et al. (1981), Carroll et al. (1998), Icenhower and Dove (2000), and Rimstidt and Barnes (1980). Icenhower and Dove's study was unique in that they used adsorption isotherms to account for acceleration of the rate of dissolution in the presence of small amounts of Na. However, this model is seldom used in mass transport and reaction routines because the adsorption formalism doesn't fit the rate laws that they generally use (Palandri and Kharaka, 2004).

Quartz Kinetics

The kinetics of quartz precipitation and dissolution are much more straight-forward, and have been studied extensively. Palandri and Kharaka (2004) list 17 studies that

they considered in choosing their rate parameters for quartz. Several of these studies concluded that dissolution rates are independent of pH in the acidic region.

Comparison of Laboratory and Field Rates

Carroll et al. (1998) conducted field and laboratory tests on silica precipitation rates in order to compare the various rates. In addition, they compared rates calculated from empirical (Bohlmann et al., 1981; Weres et al., 1982) and theoretically-based (Bird et al., 1986; Renders et al., 1995; Rimstidt and Barnes, 1980) models to rates derived from their field and laboratory experiments. They found that their field rates were within an order of magnitude of the empirical models, but were three orders of magnitude faster than those predicted by the theoretically-based models. They also found that the rate laws that match their laboratory and field data differed. They suggest that the laboratory precipitation mechanisms were elementary (i.e., simple and reversible) while the field data were dominated by surface defect and surface nucleation controls.

Chemical modeling of augmentation waters

The engineered geothermal system (EGS) program of the U.S. Department of Energy is supporting some injection permeability-enhancement research at Coso. As part of this program chemical modeling of the scale potential of injection-augmentation water was performed. This is a very synergistic task, combining the geochemical database developed under the Navy contract with modeling expertise supported by the DOE. In addition, COC has cooperated by supplying any extra data needed, such as the composition of the augmentation water. The purpose of the most recent set of simulations was to determine if acidification of groundwater prior to injection would potentially reduce carbonate scaling. The simulations indicated that a modest pH adjustment with acid would be more efficacious than mixing with condensate. This would inhibit carbonate deposition, although anhydrite precipitation would probably still occur. These results are summarized in Appendix I.

REFERENCES

Abrigo, F.V., Molling, P.A. and Acuna, J.A., 2002. Determination of recharge and cooling rates using geochemical constraints at the Mak-Ban (Bulalo) geothermal reservoir, Philippines. Geothermics, 33: 11-56.

Adams, M.C., 1994. Geochemical monitoring of the Coso geothermal system, Prepared for the Geothermal Program Office, Naval Air Weapons Station, China Lake, CA.

Adams, M.C., 1995. Geochemical monitoring of the Coso geothermal system - first out year, Prepared for the Geothermal Program Office, Naval Air Weapons Station, China Lake, CA.

Adams, M.C., Moore, J.N., Bjornstad, S., McCulloch, J. and Buck, C., 2005. Fluid-mineral equilibria and injection in EGS - effect of injecting groundwater, Thirtieth

Workshop on Geothermal Reservoir Engineering, Stanford University, Stanford, California.

Arnorsson, S., 1975. Application of the silica geothermometer in low temperature hydrothermal areas in Iceland. American Journal of Science, 275(7): 763-784.

Bird, G., Boon, J. and Stone, T., 1986. Silica transport during steam injection into oil sands. 1. Dissolution and precipitation kinetics of quartz: New results and review of existing data. Chemical Geology, 54: 69-80.

Bohlmann, E.G., Mesmer, E.G. and Berlinski, P., 1981. Silica scaling in simulated geothermal brines. ORNL/TM-7681, Oak Ridge National Laboratory.

Carroll, S., Mroczek, E., Alai, M. and Ebert, M., 1998. Amorphous silica precipitation (60 to 120oC): Comparison of field and laboratory rates. Geochemica et Cosmochimica Acta, 62(8): 1379-1396.

Chan, S.H., 1989. A review on solubility and polymerization of silica. Geothermics, 18: 49-56.

Chen, C.A. and Marshall, W.L., 1982a. Amorphous silica solubilities IV. Behavior in pure water and aqueous sodium chloride, sodium sulfate, magnesium chloride, and magnesium sulfate solutions up to 350°C. Geochemica et Cosmochimica Acta, 46: 279-287.

Chen, C.A. and Marshall, W.L., 1982b. Amorphous silica solubilities V. Predictions of solubility behavior in aqueous mixed electrolyte solutions to 300°C. Geochemica et Cosmochimica Acta, 46: 289-291.

Dunstall, M.G. and Brown, K.L., 1998. Silica scaling under controlled hydrodynamic conditions: vertical flat plate and vertical cylinder tests, Twenty-Third Workshop on Geothermal Reservoir Engineering, Stanford University, Stanford, CA, pp. 204-210.

Ellis, A.J. and Mahon, W.A.J., 1977. Chemistry and Geothermal Systems. Academic Press, New York, NY, 392 pp.

Fleming, B.A., 1986. Kinetics of reaction between silicic acid and amorphous silica surfaces in NaCl solutions. Journal of Colloid and Interface Science, 110(1): 40-64.

Fournier, R.O., 1981. Application of water geochemistry to geothermal exploration and reservoir engineering. In: L. Rybach, and Muffler, L. J. P. (Editor), Geothermal Systems: Principles and Case Histories. John Wiley & Sons, New York, pp. 109-143.

Fournier, R.O., 1983. A method of calculating quartz solubilities in aqueous sodium chloride solutions. Geochemica et Cosmochimica Acta, 47: 579-586.

Fournier, R.O. and Potter, R.W., II, 1982. A revised and expanded silica [quartz] geothermometer. Geothermal Resources Council Bulletin, 11(10): 3-12.

Fournier, R.O. and Rowe, J.J., 1966. Estimation of underground temperatures from the silica content of water from hot springs and wet-steam wells. American Journal of Science, 264: 685-697.

Fournier, R.O. and Truesdell, A.H., 1973. An empirical Na-K-Ca geothermometer for natural waters. Geochimica et Cosmochimica Acta, 37: 1255-1275.

Gallup, D.L., 1989. The solubility of amorphous silica in geothermal brines, Transactions, Geothermal Resources Council, pp. 241-245.

Gallup, D.L., 1996. Brine pH modification scale control technology, Transactions, Geothermal Resources Council, pp. 749-755.

Gallup, D.L., 1997. The interaction of silicic acid with sulfurous acid scale inhibitor. Transactions, Geothermal Resources Council, 21: 49-53.

Gallup, D.L., 2002. Investigations of organic inhibitors for silica scale control in geothermal brines. Geothermics, 31: 415-430.

Grens, J.Z. and Owen, L.B., 1977. Field evaluation of scale control methods: acidification, Transactions: Geothermal Resource Council, pp. 119-121.

Gunnarsson, I. and Arnorsson, S., 2000. Amorphous silica solubility and the thermodynamic properties of H4SiO4 in the range of 0o to 350oC at Psat. Geochemica et Cosmochimica Acta, 64: 2295-2307.

Harper, R.T. and Jordan, O.T., 1985. Geochemical changes in response to production and reinjection for Palinpinon-I geothermal field, Negros Oriental, Philippines, Proceedings of the seventh New Zealand Geothermal Workshop. University of Auckland, Auckland, New Zealand, University of Auckland, Auckland, New Zealand, pp. 39-44.

Heaney, P.J., Prewitt, C.T. and Gibbs, G.V. (Editors), 1994. Silica: Physical Behavior, Geochemistry, and Materials Applications. Reviews in Mineralogy, 29. Mineralogical Society of America, Washington, D.C.

Henley, R.H., 1984a. Aquifer boiling and excess enthalpy wells, Fluid Mineral Equilibria in Hydrothermal Systems. Reviews in Economic Geology. The Economic Geology Publishing Company, El Paso TX, pp. 143-175.

Henley, R.W., 1984b. Gaseous components in geothermal processes, Fluid Mineral Equilibria in Hydrothermal Systems. Reviews in Economic Geology. The Economic Geology Publishing Company, El Paso TX, pp. 45-54.

Hirowatari, K. and Yamachi, M., 1990. Experimental study on a scale prevention method using exhausted gases from geothermal power stations, Transactions, Geothermal Resources Council, pp. 1599-1602.

Horne, R.N., Johns, R.A., Adams, M.C., Moore, J.N. and Stiger, S.G., 1987. The use of tracers to analyze the effects of reinjection into fractured geothermal reservoirs, Geothermal Program Review V. Department of Energy, Washington, D.C., , pp. 37-52.

Icenhower, J.P. and Dove, P.M., 2000. The dissolution kinetics of amorphous silica into sodium chloride solutions: Effects of temperature and ionic strength. Geochemica et Cosmochimica Acta, 64(24): 4193-4203.

Icopini, G.A., Brantley, S.L. and Heaney, P.J., 2005. Kinetics of silica oligomerization and nanocolloid formation as a function of pH and ionic strength at 25°C. Geochemica et Cosmochimica Acta, 69: 293-303.

Iler, R.K., 1979. The chemistry of silica. John Wile and Sons, Inc., New York, NY.

Klein, C.W., 1995. Management of fluid injection in geothermal wells to avoid silica scaling at low levels of silica saturation, Transactions, Geothermal Resources Council, pp. 503-511.

Leslie, B.W. and Hammond, D.E., 1990. An investigation of water-rock interaction in an active geothermal field using uranium series isotopes, Geological Society of America - Abstracts with Programs, Boulder, CO, pp. 56.

Lovelock, B.G., 1995. Deviations in silica geothermometdry at Wairakei, World Geothermal Congress, pp. 983-988.

Malate, R.C.M. and O'Sullivan, M., 1991. Modelling of chemical and thermal changes in Well PN-26 Palinpinon Geothermal Field, Phillippines. Geothermics, 20(291-318).

Palandri, J.L. and Kharaka, Y.K., 2004. A compilation of rate parameters of water-mineral interaction kinetics for application to geochemical modeling. Open File Report 2004-1068, U.S. Geological Survey, Menlo Park, CA.

Renders, P.J.N., Gammons, C.H. and Barnes, H.L., 1995. Precipitation and dissolution rate constants for cristobalite from 150o to 300oC. Geochemica et Cosmochimica Acta, 59: 77-85.

Rimstidt, J.D., 1997. Quartz solubility at low temperatures. Geochemica et Cosmochimica Acta, 61: 2553-2558.

Rimstidt, J.D. and Barnes, H.I., 1980. The kinetics of silica-water reactions. Geochemica et Cosmochimica Acta, 44: 1683-1699.

Stefansson, V., 1997. Geothermal reinjection experience. Geothermics, 26: 99-139.

Sullera, M.M. and Horne, R.N., 1999. Inferring injection returns from chloride monitoring data, Twenty-Fourth Workshop on Geothermal Reservoir Engineering. Stanford University, Stanford Ca, Stanford University, Stanford CA.

Sullera, M.M. and Horne, R.N., 2001. Inferring injection returns from chloride monitoring data. Geothermics, 30(6): 591-616.

Weres, O., Yee, A. and Tsao, L., 1982. Equations and type curves for predicting the polymerization of amorphous silica in geothermal brine. Society of Petroleum Engineers Journal, 22: 9-16.

Zhu, C., 2005. In situ feldspar dissolution rates in an aquifer. Geochemica et Cosmochimica Acta, 69(6): 1435-1454.

Figure 1. Injection locations and quantities during 2004.
Figure 2. Location of wells that produced single-phase steam during 2004.
Figure 3. Average ratio of chloride to boron in the injection fluids during 2004.
Figure 4. Average chloride concentration(ppm) in the injection fluids during 2004.
Figure 5. NaKCa geothermometer temperatures (^{o}C) during 2004.
Figure 6. Percent change in the NaKCa geothermometer temperatures from 2003 to 2004.
Figure 7. A simple qualitative evaluation of trends in the NaKCa geothermometer temperatures in recent years.
Figure 8. A more detailed qualitative evaluation of NaKCa geothermometer temperature trends.
Figure 9. Quartz geothermometer temperatures (^{o}C) during 2004.
Figure 10. Percent change in the quartz geothermometer temperatures from 2003 to 2004.
Figure 11. A simple qualitative evaluation of trends in the quartz geothermometer temperatures in recent years.
Figure 12. A more detailed qualitative evaluation of quartz geothermometer temperature trends.
Figure 13. Excess steam fractions during 2004.
Figure 14. Percent change in the excess steam fractions from 2003 to 2004.
Figure 15. Chloride concentrations (ppm) during 2004.
Figure 16. Percent change in the chloride concentrations from 2003 to 2004.
Figure 17. Qualitative evaluation of chloride concentration trends in recent years.
Figure 18. Chloride to boron ratios during 2004.
Figure 19. Percent change in the chloride to boron ratio between 2003 and 2004.
Figure 20. A comparison of the wells in which the quartz geothermometer temperature is greater than that of NaKCa during 2004 with the 2003 data.
Figure 21. Isotopic variation of the water from well 4P-1 since 1979.
Figure 22. Isotopic variation of the water from well 4K-1 since 1993.
Figure 23. Isotopic variation of the water from well 4K-1 since 1993. Composition of rain (upper red circle) and snow (lower red circle) during Jan 2005 sampling season are shown for comparison.
Figure 24. Isotopic variation of steam and liquid from Devil's Kitchen since 1974.
Figure 25. Isotopic variation of the water from the Nicol Prospect since 1974.
Figure 26. Isotopic variation of the mudpots and pools along the Coso Fault since 1974.
Figure 27. Isotopic variation of the water from West Canyon since 1993.
Figure 28. Isotopic variation of the South Pool since 1989.
Figure 29. Isotopic variation of the Navy II fumarole since 1995.
Figure 30. Schematic representation of how elevated silica concentrations may precede thermal breakthrough of injection water. The graph is a plot of temperature versus saturation for typical injection waters.

Appendix I - Summary of the Conductive Heating Results

Results of the simulations in which groundwater was heated with acid addition and with condensate addition were examined. Figure 1 shows the effects of heating with no acidification or condensate addition, figures 2-4 show the effects of acidification, and figures 5-7 show the effects of condensate addition. The waters were heated from 20° to 300°C with no mixing, and precipitation was allowed.

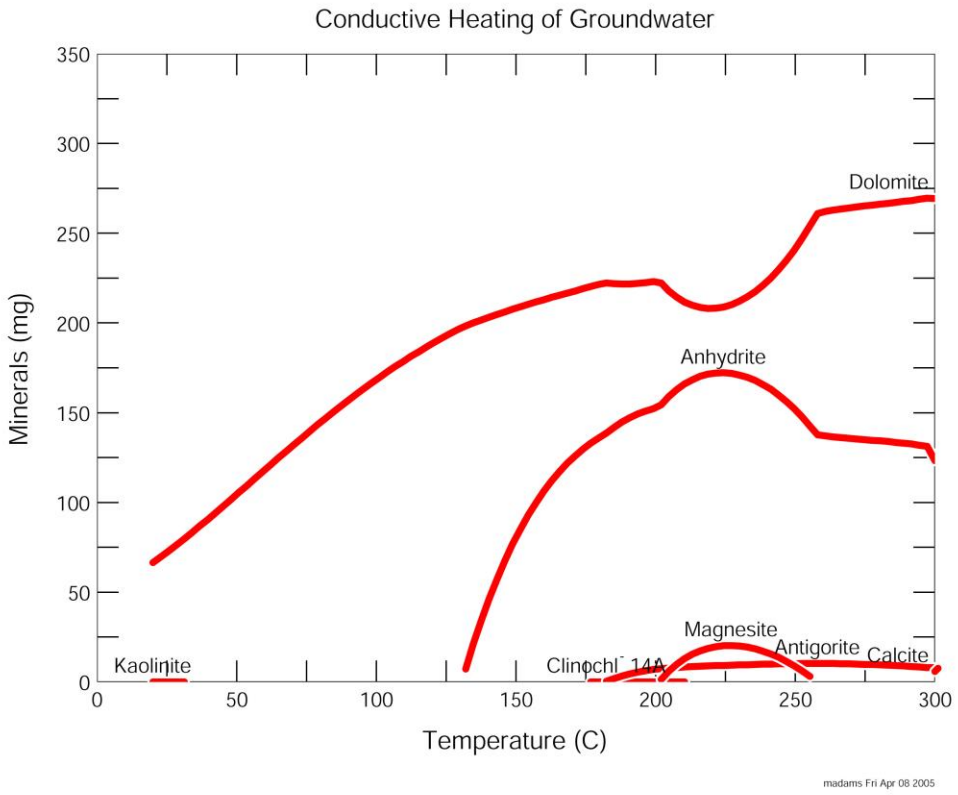

Figure 1. Groundwater conductively heated from 20° to 300°C.

It can be seen in figure 1 that precipitation of dolomite starts immediately upon heating. The other major precipitating mineral is anhydrite, which does not start precipitating until the temperature has reached approximately 130°C. As discussed in Adams (2005), dolomite may be kinetically inhibited and calcite may precipitate instead. Simulations were also run in which dolomite was inhibited, but are not shown in this report for the sake of brevity.

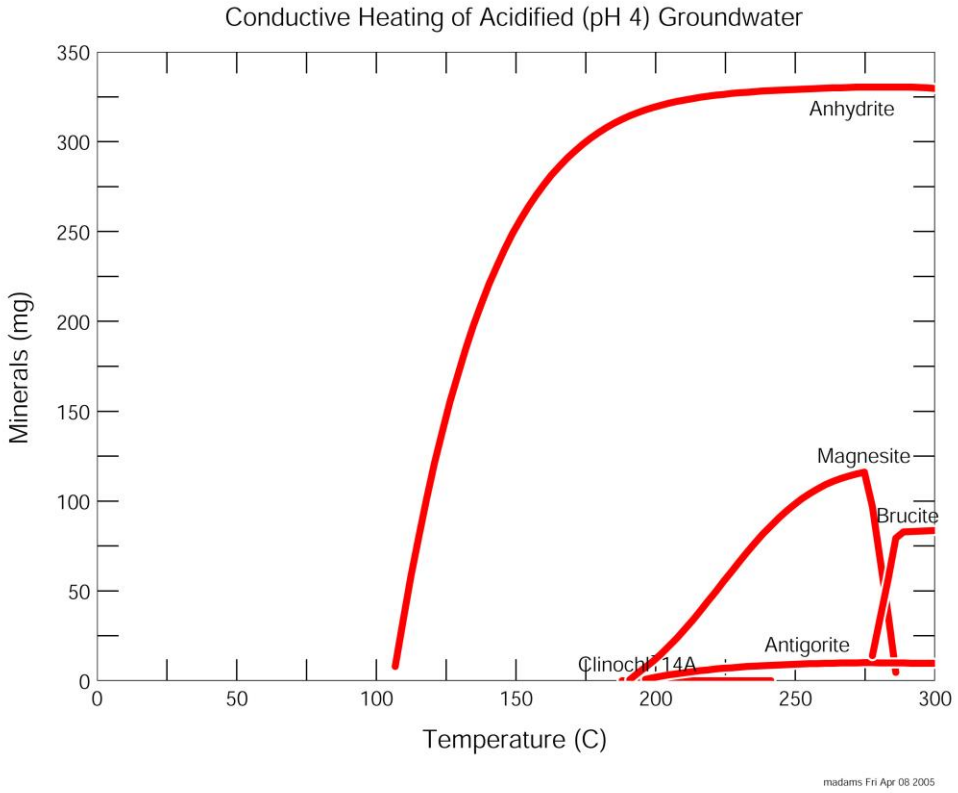

Figure 2. Groundwater acidified to a pH of 4 and then conductively heated from 20° to 300°C.

Acidification to a pH of 4 completely prevented the precipitation of carbonates. The initiation of anhydrite precipitation moves to a slightly lower temperature.

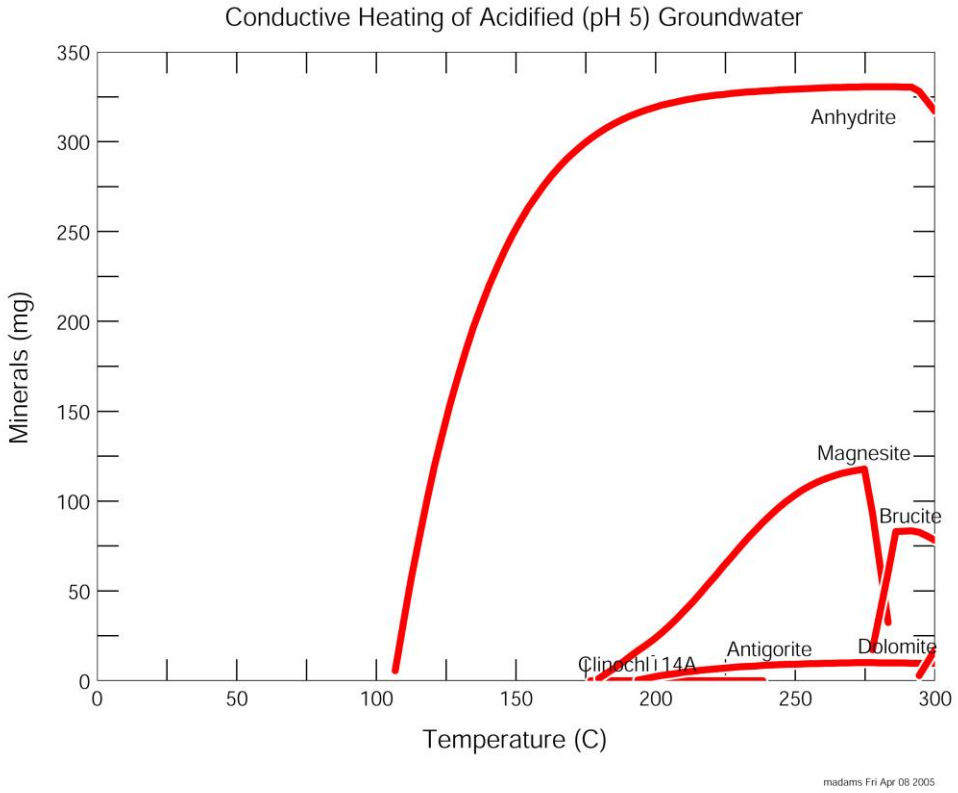

Figure 3. Groundwater acidified to a pH of 5 and then conductively heated from 20° to 300°C.

Acidification to a pH of 5 also prevented the precipitation of carbonates until high temperatures were reached. The attainment of such high temperatures is unlikely without mixing occurring. The initiation of anhydrite precipitation again moves to a slightly lower temperature.

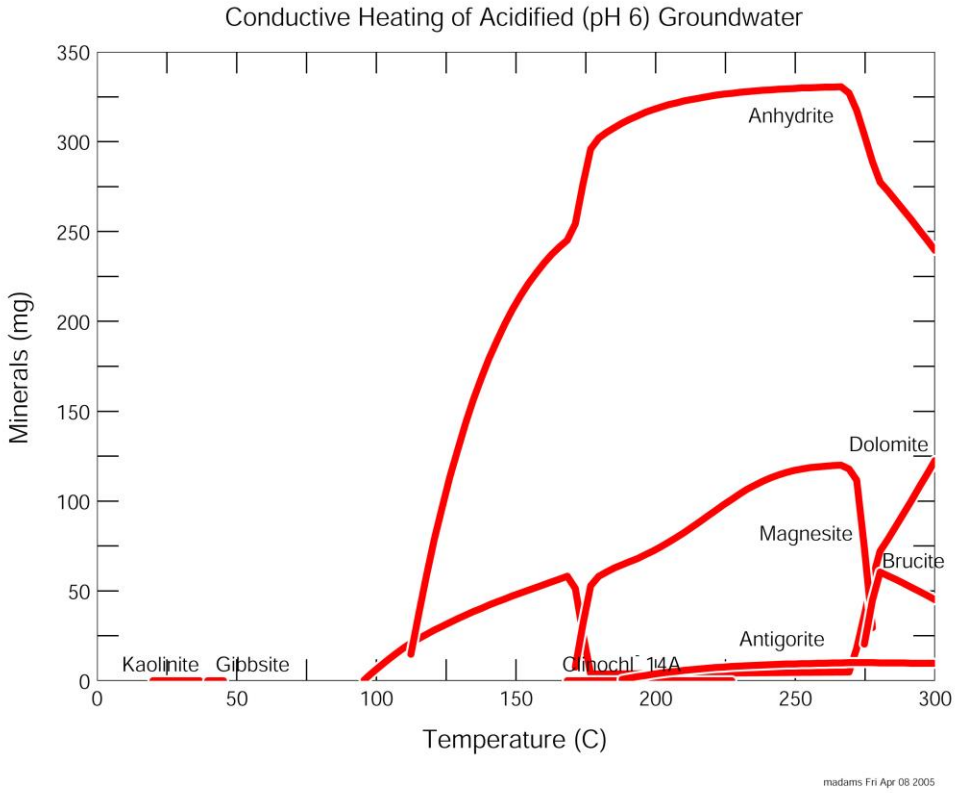

Figure 4. Groundwater acidified to a pH of 6 and then conductively heated from 20° to 300°C.

Acidification to a pH of 6 prevents Ca and Mg mineral precipitation below a temperature of 100°C. This may be sufficient to move the precipitation out into the formation. The initiation of anhydrite precipitation occurs at a similar temperature at this pH.

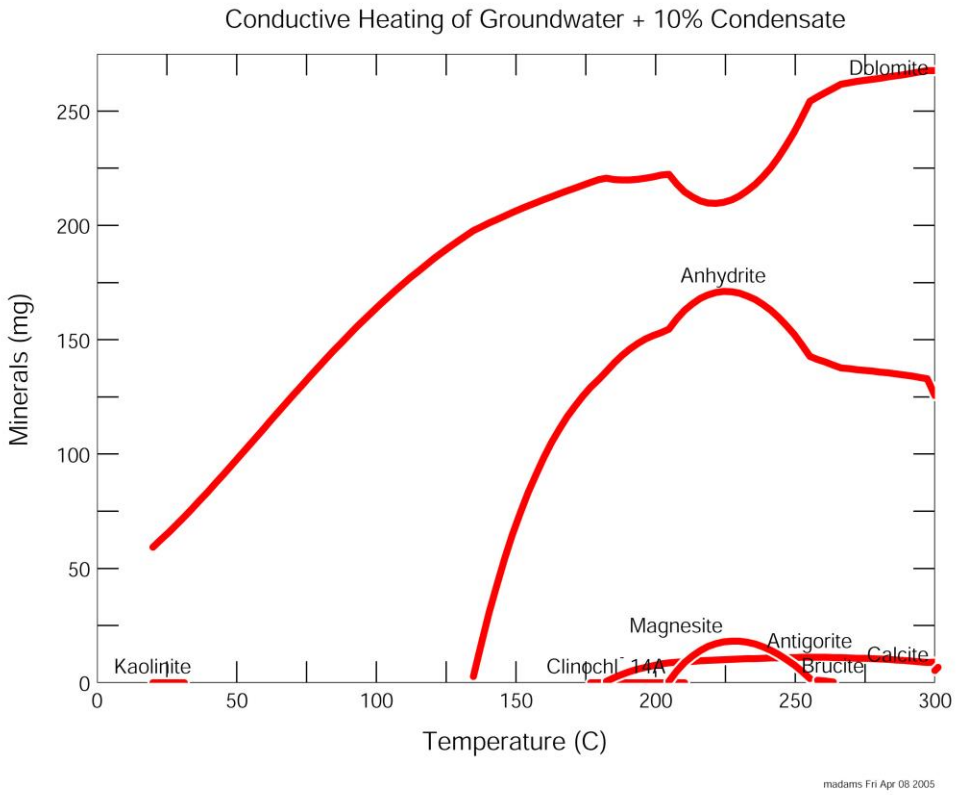

Figure 5. Conductive heating of a mixture of groundwater and 10% condensate.

Simulations were also run in which the groundwater was mixed with condensate. Figure 5 shows a mixture with 10% condensate. The results are very nearly identical to the simulation in which pure groundwater was heated.

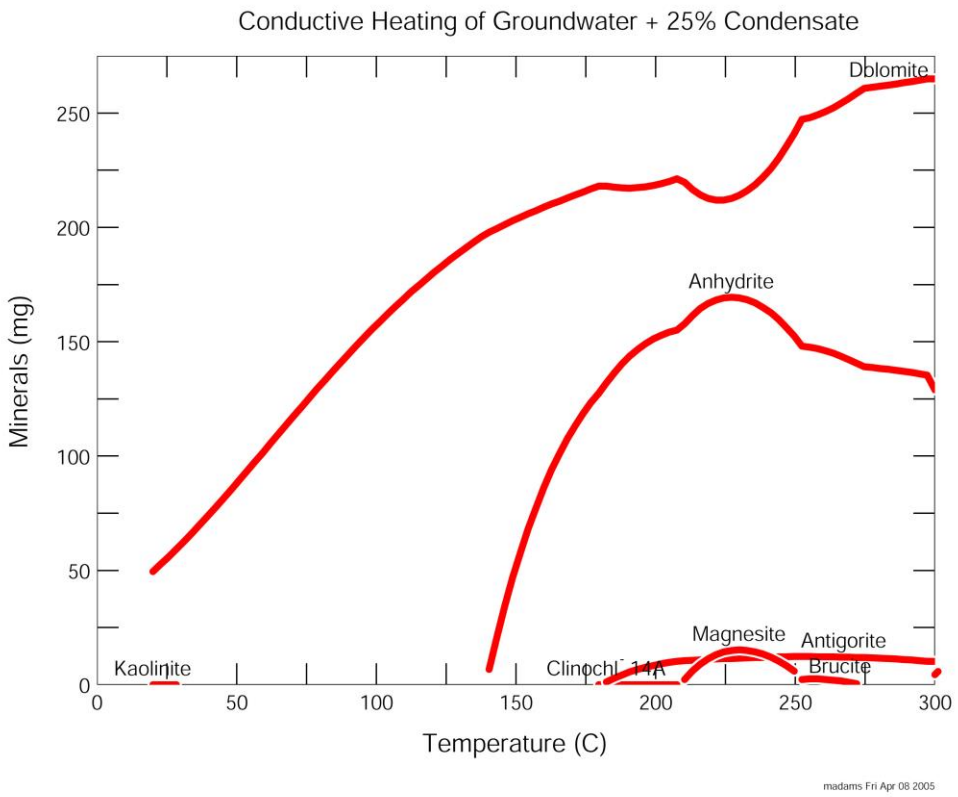

Figure 6. Conductive heating of a mixture of groundwater and 25% condensate.

A similar pattern was observed for the addition of 25% condensate.

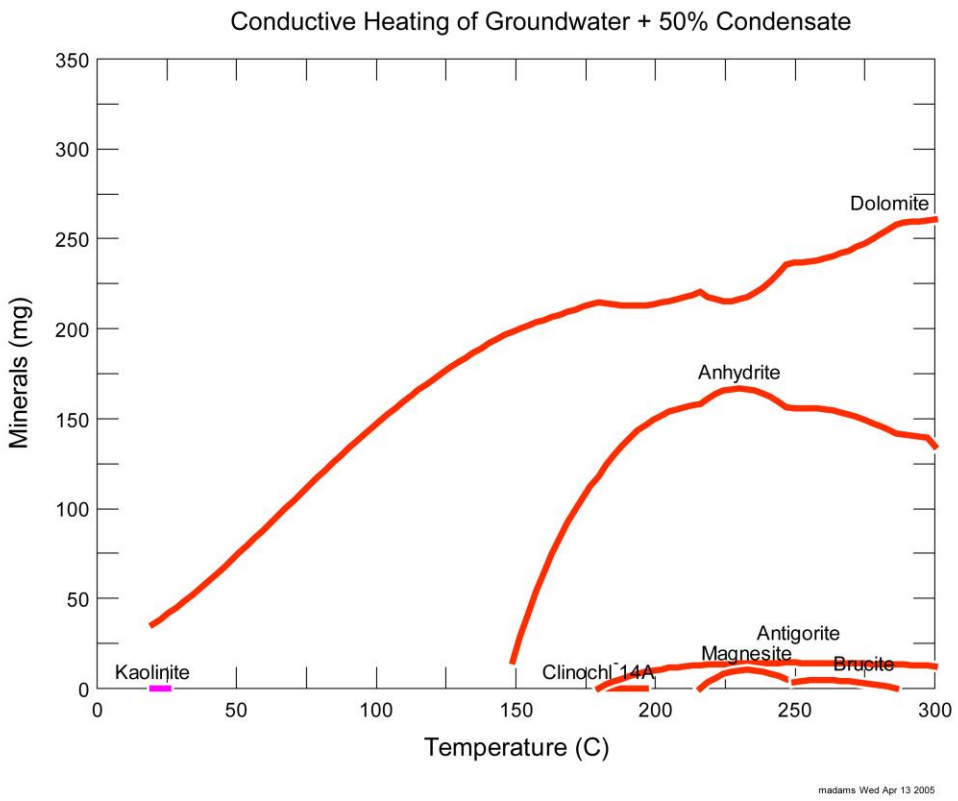

Figure 7. Conductive heating of a mixture of groundwater and 50% condensate.

Little affect was observed with the addition of 50% condensate. Acidification, even to a pH as high as 6, appears to be the most efficient option for avoiding well bore scale under the conditions simulated.